SCIENTIFIC REPORTS

OPEN

# Gas Sensing Properties of Epitaxial $LaBaCo_2O_{5.5+\delta}$ Thin Films

M. Liu[1], S. P. Ren[1], R. Y. Zhang[1], Z. Y. Xue[1], C. R. Ma[2], M. L. Yin[3], X. Xu[4], S. Y. Bao[4] & C. L. Chen[4,5]

Received: 20 January 2015
Accepted: 01 May 2015
Published: 06 July 2015

**Chemical reactivity and stability of highly epitaxial mixed-conductive $LaBaCo_2O_{5.5+\delta}$ (LBCO) thin films on (001) $LaAlO_3$ (LAO) single-crystalline substrates, fabricated by using pulsed laser deposition system, were systematically investigated. Microstructure studies from x-ray diffraction indicate that the films are *c*-axis oriented with the interface relationship of $[100]_{LBCO}//[100]_{LAO}$ and $(001)_{LBCO}//(001)_{LAO}$. LBCO thin films can detect the ethanol vapor concentration as low as 10ppm and the response of LBCO thin film to various ethanol vapor concentrations is very reliable and reproducible with the switch between air and ethanol vapor. Moreover, the fast response of the LBCO thin film, as the *p*-type gas sensor, is better than some *n*-type oxide semiconductor thin films and comparable with some nanorods and nanowires. These findings indicate that the LBCO thin films have great potential for the development of gas sensors in reducing/oxidizing environments.**

Cobalt-based oxides have attracted scientists and engineers much attention due to their unique magnetic, electrical transport and optical properties, which have been used to design various new concept devices, such as solid state fuel cell, energy harvest, gas sensors, etc[1–10]. Among them, the oxygen-deficient double perovskite cobaltates, $LaBaCo_2O_{5.5+\delta}$ (LBCO), show particularly interesting phenomena with the A-site order, nanoscale order, and disorder structures, such as, different spin state configurations, giant MR effect, etc[11–16]. To under these physics nature, single crystalline LBCO thin films are required. Recently, highly epitaxial single crystalline LBCO thin films were fabricated on various substrates, such as (001) $LaAlO_3$ (LAO)[16], (001) $SrTiO_3$[17–19], (001) MgO[20,21], and (110) $NdGaO_3$[22]. The LBCO films not only exhibit a much larger magnetoresistance value than those from various phases of its bulk material, but also possess an extraordinary sensitivity to $H_2$ and $O_2$, especially an exceedingly fast redox reaction at high temperature and a superfast oxygen vacancy exchange diffusion chemical dynamics[16,23]. Therefore, the LBCO thin films are one promising candidate for the development of the gas sensors in reducing/oxidizing environments, which is one of the critical research issues in the public safety and energy security.

Gas-sensing materials using the *n*-type oxide semiconductor have been intensively studied, such as ZnO[24,25], $TiO_2$[26–28], SnO[29–31], $WO_3$[32], $Fe_2O_3$[33–35], $In_2O_3$[36], *etc*. However, there are very few reports on the gas-sensing materials using *p*-type oxide semiconductor, such as NiO[37–39], CuO[40], $LaFeO_3$[41], $Co_3O_4$,[42–55] LBCO[16,23]. Compared with n-type oxide semiconductor for gas-sensing, the p-type oxide semiconductors with distinctive surface reactivity and oxygen adsorption can enhance gas selectivity, decrease the dependence of humidity to negligible level and improve the recovery speed, reviewed by Kim and Lee[46]. Also, it is a good catalyst to promote selective oxidation of various volatile organic compounds[47–50].

Various oxidation states ($Co^{2+}$ /$Co^{3+}$ /$Co^{4+}$) of cobalt in LBCO thin film make it to be a good candidate as *p*-type gas sensor. The conductivity is strongly dependent on the valence states, which can change the LBCO from good conductive to insulate. Ideally, when the valence states are all $Co^{+3}$, the LBCO

[1]Electronic Materials Research Laboratory, Key Laboratory of the Ministry of Education & International Center for Dielectric Research, Xi'an Jiaotong University, Xi'an 710049, People's Republic of China. [2]State Key Laboratory for Mechanical Behavior of Materials, Xi'an Jiaotong University, Xi'an 710049, People's Republic of China. [3]School of Science, Xi'an Technological University, Xi'an 710032, P. R. China. [4]Department of Physics and Astronomy, University of Texas at San Antonio, TX 78249, United States. [5]The Texas Center for Superconductivity, University of Houston, Houston, Texas 77204, United States. Correspondence and requests for materials should be addressed to M.L. (email: m.liu@mail.xjtu.edu.cn) or C.L.C. (email: cl.chen@utsa.edu)

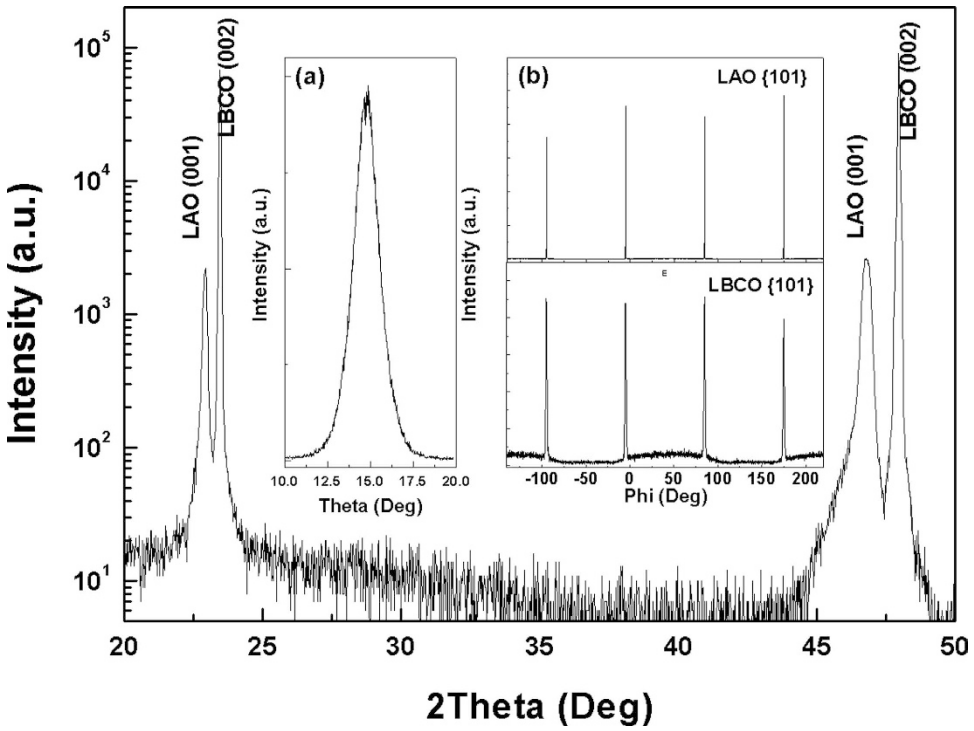


**Figure 1. Typical XRD pattern of the LBCO films grown on (001) LAO substrates** . The inset is (**a**) rocking curve from the (002) reflection for the LBCO film and (**b**) the $\phi$ scans taken around the {101} diffraction of the LBCO film and LAO substrate.

should be insulate. And when the valence states are mixed with $Co^{+3}$ and $Co^{+4}$ or $Co^{+2}$ and $Co^{+3}$, the LBCO should be semiconductor or semimetallic, respectively. Since the LBCO films were grown in the pure oxygen of 250 mTorr, the films are good conductive. Moreover, the $Co^{+4}$ is not as stable as $Co^{+3}$. Therefore, the valence states should be a mixed state of $Co^{+3}$ and $Co^{+4}$. When LBCO thin film is exposed to the reducing gas, parts of $Co^{+4}$ changed into $Co^{+3}$ and the resistance increases. In the contrast, the gas change to oxidizing gas, parts of $Co^{+3}$ changed into $Co^{+4}$ and the resistance decreases[51,52]. Ethanol vapor is safer and more active than other gas, such as $H_2$, ammonia, hydrogen sulfide, which is used as the representative of reducing gases. In this paper, we explore here the transient responses of the LBCO thin films to various ethanol vapor concentrations at different operating temperatures. It was found that even though ethanol vapor concentration is as low as 10 ppm, the LBCO thin film still can detect the transient response. Moreover, the response time can be reduced to ~24 s under the ethanol vapor concentration of 400 ppm with the recovery time of only ~10 s at 375 °C. These results indicate that the LBCO thin films have great potential for the development of the gas sensor applications in reducing/oxidizing environments, expect the applications on giant magnetoresistance and cathode for solid oxide fuel cell.

## Results and Discussion

The crystalline quality of the LBCO thin films was characterized by the XRD $\theta-2\theta$ scan, rocking curve, $\phi$ scan and reciprocal space mappings (RSMs). Figure 1 is a typical $\theta-2\theta$ pattern for the LBCO thin films on (001) LAO substrates showing that only the (00*l*) peaks can be detected for the LBCO thin films. It is revealed that the films are *c*-axis oriented or the *c*-axis normal to the substrate surface. The rocking curve measurements from the (002) reflections for the LBCO films show that the Full Width of Half Maximum (FWHM) is ~0.92°, as shown in the inset (a) of Fig. 1, indicating that the LBCO films on LAO substrates have good crystalline quality. To understand the in-plane interface relationships between the LBCO films and the LAO substrates, the $\phi$ scans measurements have been performed. The inset (b) of Fig. 1 is the $\phi$ scans taken around from the {101} reflections of the LBCO films and LAO substrates. The four-fold symmetry and sharp peaks in the $\phi$ scan suggest that the films have good epitaxial nature. Therefore, the orientation relationships between the thin films and the substrates can be determined to be $[100]_{LBCO}//[100]_{LAO}$ and $(001)_{LBCO}//(001)_{LAO}$. RSMs is a very effective method to study the microstructure information, such as lattice parameters, defect density, domain structure, etc. in order to obtain the lattice parameters and interface strain of LBCO films on LAO substrates, the RSMs have been performed taken around from the symmetric (002) and asymmetric (103) reflections of the LBCO films and LAO substrates, as shown in the Fig. 2. According to the Bragg law and the angles' relationship between these crystalline planes, the in-plane (*a* & *b*) abd out-of–plane (*c*) lattice parameters of LBCO films on LAO

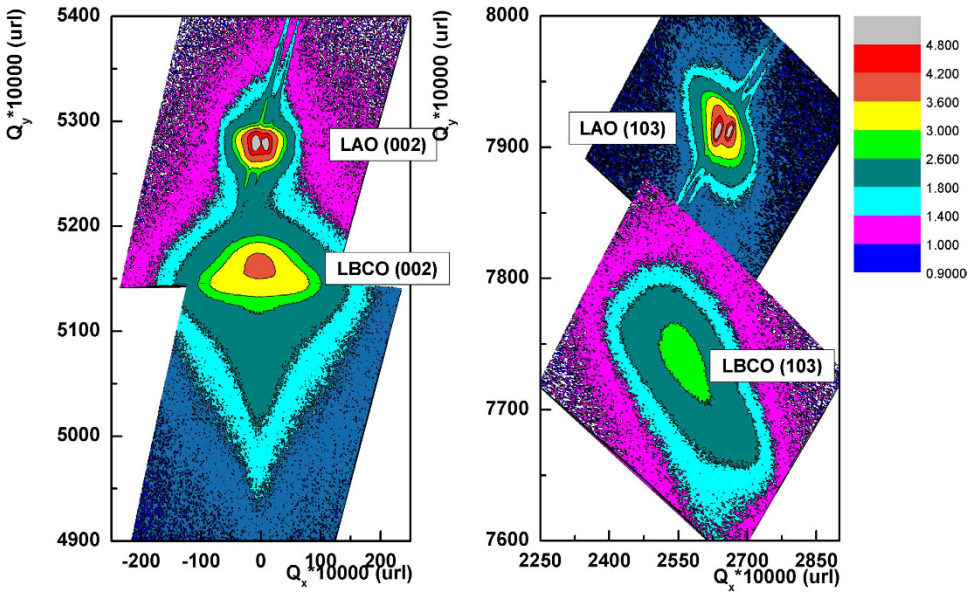


**Figure 2.** Reciprocal space mappings taken around from the symmetric (002) and asymmetric (103) reflections of the LBCO films and LAO substrates.

substrates can be calculated from the RSMs. The in-plane and out-of-plane lattice parameter is 3.90 Å and 3.88 Å, respectively. It is shown that this LBCO film on LAO is full relaxation state.

In order to identify the optimum working temperature for the LBCO gas sensors, the sensing transient response of the LBCO films to 1000 ppm ethanol vapor exposure were investigated as a function of sensor temperature from 250 °C to 450 °C, as shown in the Fig. 3(a). It is clearly seen that the resistance of LBCO thin film increase when it is exposed to the ethanol vapor (reducing gas), then the resistance decrease when the gas change from 1000 ppm ethanol vapor to air, which is in agreement with our previous studies under the gas switch between $H_2$ and $O_2$[16,23]. In fact, the LBCO thin films will generate a high density of oxygen vacancies when it is exposed to the reducing gas[53], such as ethanol vapor gas. This chemical processing can be represented by:

$$C_2H_5OH(gas) + 6O^{2-} \rightarrow 2CO_2(gas) + 3H_2O(gas) + 6e^-$$

The electrons are released into the LBCO films through the oxidation reactions with ethanol vapor reducing gas. Thus, the increased electronic density will result in the increase of the resistance due to the LBCO films are p-type semiconductors, On the other hand, the resistances of the LBCO thin films will decrease when exposed to oxidizing gas, such as air. The response time from air to 1000 ppm ethanol vapor decrease with the temperature increase. Especially, the response time rapidly drop and become faster when the temperature exceed to 375 °C. Although the LBCO thin films can detect ethanol gas at the temperature of 250 °C and 300 °C, the resistance of LBCO thin film can't recovery completely in short time when it exposed to air. Thus, the working temperature above 300 °C is better for the excellent performance as ethanol/reducing gas sensor. Meanwhile, the stability of the LBCO thin film as ethanol/reducing gas sensor has been examined, as shown in Fig. 3(b). The response and recovery repeatability of the LBCO thin film is examined under 1000 ppm ethanol vapor at 375 °C. It shows that the resistance change of LBCO thin film can keep its initial value after circle operation, revealing that the LBCO thin film as ethanol/reducing gas sensor have good reproducibility.

To investigate the sensitivity of LBCO thin film as ethanol gas sensor, the transient response or the resistance switching behavior during the change between air and various ethanol vapor concentrations at 375 °C was examined. As shown in the Fig. 4, the LBCO thin films have reliable and reproducible responses during the change between air and various ethanol vapor concentrations. Even at very low concentration of 10 ppm, the LBCO films still can detect transient response. The ratio of resistance switching between air to ethanol vapor is strongly dependent upon the ethanol vapor concentrations, or linearly-like increases with the increase of the ethanol vapor partial pressures from 10 ppm to 5000 ppm, as seen in the inset of Fig. 4. The sensitivity ($S$) of the LBCO thin film as the ethanol gas sensor increase form 1.04 at 10 ppm to 2.92 at 5000 ppm. The $S$ determined by using the formula $S = R_g/R_a$, where $R_a$ and $R_g$ are resistance of the gas sensor in air and in testing gas atmosphere, respectively. The sensitivity can be enhanced by replacing the air with oxygen gas.

It is known that the response and recovery times are the two important quantity factors for the gas sensors, As shown in the inset of Fig. 5, the response time is the time taken by the resistance change from

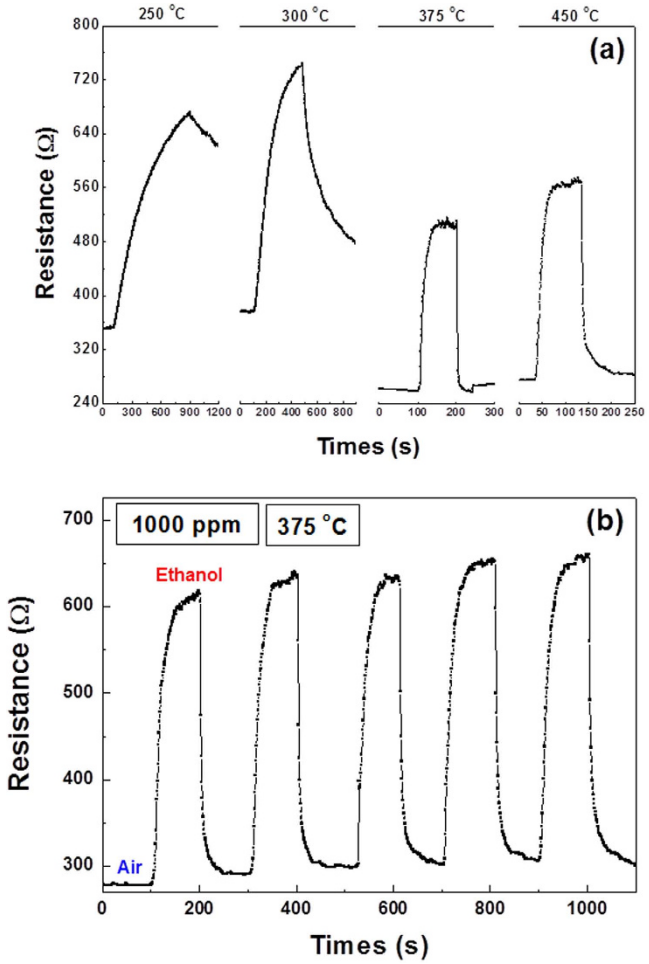


**Figure 3.** (**a**) Transient responses at different temperatures from 250 to 450 °C, (**b**) transient response vs . number of exposure tests during the change of air to 1000 ppm ethanol vapor concentration at 375 °C.

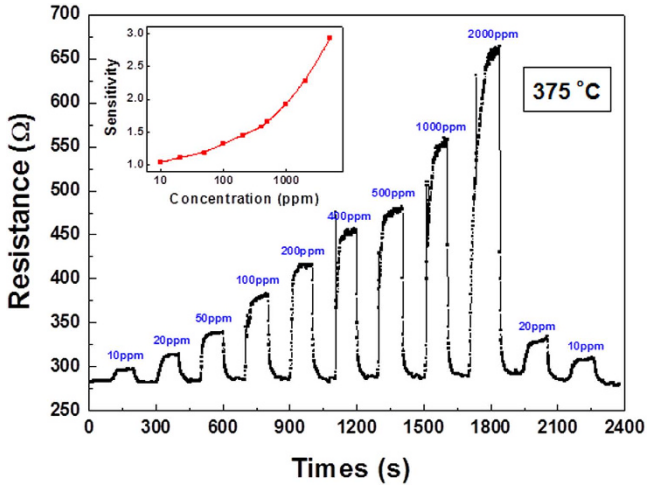


**Figure 4.** Transient responses and the sensitivity (inset) of the LBCO gas sensors during the change of air to various ethanol vapor concentrations at 375 °C.

$R_{air}$ to $R_{air}+[R_{gas}-R_{air}]*90\%$, and the recovery time is the time taken by the resistance change from $R_{gas}$ to $R_{gas}-[R_{gas}-R_{air}]*90\%$. The response and recovery factors for the LBCO thin films as ethanol gas sensors are shown in Fig. 5 and Table 1. The response time decreases from ~34 s (10 ppm) to ~24 s (400 ppm)

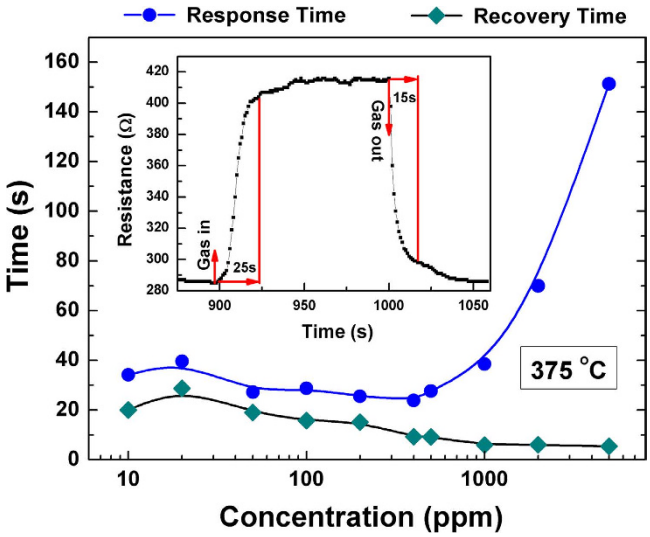


**Figure 5.** The plot of response time and recovery time of the LBCO gas sensors during the change of air to various ethanol vapor concentrations at 375 °C, the inset shows the definition of the response and recovery times.

| Ethanol vapor concentrations(ppm) | Sensitivity | Response time(s) | Recovery time(s) |
|---|---|---|---|
| 10 | 1.04 | 34 | 20 |
| 20 | 1.11 | 40 | 29 |
| 50 | 1.19 | 27 | 19 |
| 100 | 1.33 | 29 | 16 |
| 200 | 1.45 | 26 | 15 |
| 400 | 1.58 | 24 | 9 |
| 500 | 1.65 | 28 | 9 |
| 1000 | 1.92 | 38 | 6 |
| 2000 | 2.28 | 70 | 6 |
| 5000 | 2.92 | 151 | 5.5 |

**Table 1.** Sensitivity, response time and recovery time for the LBCO film gas sensors under during the change of air to various ethanol vapor concentrations at 375 °C.

with the increase of ethanol vapor concentrations. Then, the response time increases with the increase of the ethanol vapor partial pressures from 500 ppm to 2000 ppm. Therefore, the optimum response time is ~24 s at the concentration of 400 ppm. The reason for the phenomena is still unclear and will be explored in the following work. There is no transition for the recovery time, which decreases from ~29 s (10 ppm) to ~6 s (2000 ppm) with the increase of the ethanol vapor concentration. Compared with some ethanol sensors, epitaxial LBCO thin film exhibits better quality factors. Table 2 gives the as-reported response times of various ethanol sensors at intermediate temperature ranges. Obviously, the response (recovery) time of the LBCO epitaxial thin films is less than that from the *n*-type gas sensors based on the NiO thin films, $SnO_2$ thin film and $TiO_2$ thick films. Normally, the response of *p*-type oxide semiconductor gas sensor is slower than *n*-type semiconductor gas sensor[54]. Moreover, it is comparable with the ZnO nanorods, CuO microsphere, hollow sea urchin-like structure $\alpha$-$Fe_2O_3$ and various nanostructure $Co_3O_4$ listed in the Table 2. Nanorods and nanowires normally have fast response due to the large reactivity area. The comparable fast response in LBCO thin films indicates that epitaxial LBCO thin films will be an good gas sensor for reducing gas, especially for ethanol vapor. The response and recovery time definitely can be improved by adjusting the nanostructure of LBCO, like LBCO nanorods and nanowires. Therefore, LBCO materials have great potential for the development of the application of gas sensors in reducing/oxidizing environments.

In summary, the sensing transient response of the epitaxial LBCO thin films during the changes of air to various ethanol vapor exposure have been investigated in the temperature range of 250 °C to 450 °C. It is shown that the LBCO thin films have reliable and reproducible responses to ethanol vapor,

| Materials | Ethanol Concentration(ppm) | Working Temperature(°C) | Response Time(s) | Recovery Time(s) | Reference |
|---|---|---|---|---|---|
| LBCO Thin Films | 100 | 375 | 29 | 16 | This paper |
| $Co_3O_4$ Nanofibers | 100 | 336 | 22.7 | 2.4 | 43 |
| $Co_3O_4$: Nanosheets, Nanorods, Nanocubes | 100 | 400 | 66, 29, 49 | 10–13 | 45 |
| $\alpha$-$Fe_2O_3$ Hollow Sea Urchin-like Structures | 21–2100 | 350 | 7–21 | 11–14 | 35 |
| CuO Microsphere | 200 | 400 | 9–17 | 4–17 | 40 |
| NiO: Thin Films, Hollow Hemispheres | 100 | 300 | 62, 49 | 47, 42 | 39 |
| ZnO Nanorods | 100 | 370 | 22 | 27 | 25 |
| $TiO_2$ Thick Films | 300 | 350 | 128 | 348 | 28 |
| $SnO_2$ Thin Film | 1250 | 350 | 42 | 88 | 31 |

**Table 2.** Comparison of Various Oxide Semiconductors in Ethanol Vapor Sensing.

even at very low concentration of 10 ppm. The optimum response time is ~24 s under the ethanol vapor concentration of 400 ppm with the recovery time of ~10 s at 375 °C. The performance of epitaxial LBCO thin film as the ethanol vapor sensor is better than that of some *n*-type oxide semiconductor thin films and comparable to that of the nanorods and nanowires structure. It is revealing that the LBCO thin films can be a promising candidate as gas sensor in reducing/oxidizing environments.

## Methods

**Film preparation.** A KrF excimer pulsed laser deposition system with a wavelength 248 nm was used to fabricate the LBCO thin films on (001) LAO single-crystalline substrates. Details of the processing conditions can be found in the related literatures[17]. Briefly, the films were grown under an oxygen pressure of 250 mTorr at 700 °C with the laser energy density of about 2.0 J /$cm^2$ at 10 Hz. The typical film thickness is about ~200 nm with the growth rate of ~13.3 nm/min. After growth the films were annealed at 700 °C for 15 min in pure oxygen (200 Torr) and then cooled down to room temperature at the rate of 30 °C/min.

**Structural and electrical characterization.** The crystalline quality and epitaxial behavior of the LBCO thin films were characterized by high-resolution x-ray diffraction (HRXRD) using PANalytical X'Per MRD. The LBCO thin films have been used for the gas sensing measurements. The ethanol sensing properties of the LBCO thin films were systematically studied using the GS-1TP intelligent gas sensing analysis system (Beijing Elite Tech. Co. Ltd., China)[55]. This analysis system consists of several parts: a heating system, gas distribution system, probe system, vacuum system, measurement system and related control software. The samples can be heated up to 500 °C with a precision of 1 °C. In order to obtain the accurate data, all the samples will be preheated at the working temperature for ~20 min. Once the LBCO gas sensors were stable, the ethanol gas will be injected into the test chamber. After the resistance of the LBCO gas sensor reaches a new constant value, we will open the test chamber to recover LBCO sensor into the air atmosphere.

## References


1. Jacobson, A. J. Materials for Solid Oxide Fuel Cells. *Chem. Mater.* **22,** 660–674 (2010).
2. DeSouza, R. A. & Kilner, J. A. Oxygen Transport in $La_{1-x}Sr_xMn_{1-y}Co_yO_{3-\delta}$ Perovskites - Part I. Oxygen Tracer Diffusion. *Solid State Ion.* **106,** 175–187 (1998).
3. Post, M. L. *et al.* Material Chemistry of Perovskite Compounds as Chemical Sensors. *Sens. Actuators B: Chem.* **59,** 190–194 (1999).
4. Wang, S. *et al.* The Effect of the Magnitude of the Oxygen Partial Pressure Change in Electrical Conductivity Relaxation Measurements: Oxygen Transport Kinetics in $La_{0.5}Sr_{0.5}CoO_{3-\delta}$ *Solid State Ion.* **140,** 125–131 (2001).
5. Luo, G. P. *et al.* Electrical and Magnetic Properties of $La_{0.5}Sr_{0.5}CoO_3$ Thin Films. *Appl. Phys. Lett.* **76,** 1908–1910 (2000).
6. Taskin, A. A. *et al.* Achieving Fast Oxygen Diffusion in Perovskites by Cation Ordering. *Appl. Phys. Lett.* **86,** 091910 (2005).
7. Kim, G. *et al.* Oxygen Exchange Kinetics of Epitaxial $PrBaCo_2O_{5+\delta}$ Thin Films. *Appl. Phys. Lett.* **88,** 024103 (2006).
8. Kim, G. *et al.* Rapid Oxygen Ion Diffusion and Surface Exchange Kinetics in $PrBaCo_2O_{5+x}$ with A Perovskite Related Structure and Ordered A Cations. *J. Mater. Chem.* **17,** 2500–2505 (2007).
9. Yuan, Z. *et al.* Epitaxial Behavior and Transport Properties of $PrBaCo_2O_5$ Thin Films on (001) $SrTiO_3$. *Appl. Phys. Lett.* **90,** 212111 (2007).
10. Fauth, F. *et al.* Interplay of Structural, Magnetic and Transport Properties in The Layered Co-based Perovskite $LnBaCo_2O_5$ (Ln = Tb, Dy, Ho). *Eur. Phys. J. B* **21,** 163–174 (2001).
11. Fauth, F. *et al.* Intermediate Spin State of $Co^{3+}$ and $Co^{4+}$ Ions in $La_{0.5}Ba_{0.5}CoO_3$ Evidenced by Jahn-Teller Distortions. *Phys. Rev. B* **65,** 060401/1–4 (2002).
12. Nakajima, T. *et al.* New A-site Ordered Perovskite Cobaltite $LaBaCo_2O_6$: Synthesis, Structure, Physical Property and Cation Order-Disorder Effect. *J. Phys. Soc. Jpn.* **74,** 1572–1577 (2005).

13. Kundu, A. K. *et al.* Spin-Locking Effect in The Nanoscale Ordered Perovskite Cobaltite $LaBaCo_2O_6$. *Phys. Rev. B* **76,** 184432 (2007).
14. Rautama, E. L. *et al.* Cationic Ordering and Microstructural Effects in The Ferromagnetic Perovskite $La_{0.5}Ba_{0.5}CoO_3$: Impact Upon Magnetotransport Properties. *Chem. Mater.* **20,** 2742–2750 (2008).
15. Rautama, E. L. *et al.* New Member of the "112" Family, $LaBaCo_2O_{5.5}$: Synthesis, Structure, and Magnetism. *Chem. Mater.* **21,** 102–109 (2009).
16. Liu, J. *et al.* Epitaxial Nature and Transport Properties in $(LaBa)Co_2O_{5+\delta}$ Thin Films. *Chem. Mater.* **22,** 799–802 (2010).
17. Liu, M. *et al.* Magnetic and Transport Properties of Epitaxial $(LaBa)Co_2O_{5.5+\delta}$ Thin Films on (001) $SrTiO_3$. *Appl. Phys. Lett.* **96,** 132106 (2010).
18. Ma, C. R. *et al.* M. H. Magnetic and Electrical Transport Properties of $LaBaCo_2O_{5.5+\delta}$ Thin Films on Vicinal (001) $SrTiO_3$ Surfaces. *ACS Appl. Mater. Interfaces* **5,** 451–455 (2013).
19. Zou, Q. *et al.* Step Terrace Tuned Anisotropic Transport Properties of Highly Epitaxial $LaBaCo_2O_{5.5+\delta}$ Thin Films on Vicinal $SrTiO_3$ Substrates. *ACS Appl. Mater. Interfaces* **6,** 6704–6708 (2014).
20. Liu, M. *et al.* Giant Magnetoresistance and Anomalous Magnetic Properties of Highly Epitaxial Ferromagnetic $(LaBa)Co_2O_{5.5+\delta}$ Thin Films on (001) MgO. *ACS Appl. Mater. Interfaces* **4,** 5524–5528 (2012).
21. Ma, C. R. *et al.* Interface Effects on the Electronic Transport Properties in Highly Epitaxial $LaBaCo_2O_{5.5+\delta}$ Films. *ACS Appl. Mater. Interfaces* **6,** 2540–2545 (2014).
22. Liu, M. *et al.* Strain-Induced Anisotropic Transport Properties of $(LaBa)Co_2O_{5+\delta}$ Thin Films on $NdGaO_3$ Substrates. *ACS Appl. Mater. Interfaces* **6,** 8526–8530 (2014).
23. Liu, J. *et al.* PO2 Dependant Resistance Switch Effect in Highly Epitaxial $(LaBa)Co_2O_{5+\delta}$ Thin Films. *Appl. Phys. Lett.* **97,** 094101 (2010).
24. Tarwal, N. L. *et al.* A Selective Ethanol Gas Sensor Based on Spray-Derived Ag-ZnO Thin Films. *J. Mater. Sci.* **48,** 7274–7282 (2013).
25. Yin, M. L. *et al.* Development of an Alcohol Sensor Based on ZnO Nanorods Synthesized Using a Scalable Solvothermal Method. *Sens. Actuators B: Chem.* **185,** 735–742 (2013).
26. Nisar, J. *et al.* $TiO_2$-Based Gas Sensor: A Possible Application to $SO_2$. *ACS Appl. Mater. Interfaces* **5,** 8516–8522 (2013).
27. Hu, P. G. *et al.* Enhancement of Ethanol Vapor Sensing of $TiO_2$ Nanobelts by Surface Engineering. *ACS Appl. Mater. Interfaces* **11,** 3263–3269 (2010).
28. Cheng, X. L. *et al.* Ag Nanoparticles Modified $TiO_2$ Spherical Heterostructures with Enhanced Gas-Sensing Performance. *Sens. Actuators B: Chem.* **155,** 716–722 (2011).
29. Yuasa, M. *et al.* Preparation of a Stable Sol Suspension of Pd-Loaded $SnO_2$ Nanocrystals by a Photochemical Deposition Method for Highly Sensitive Semiconductor Gas Sensors. *ACS Appl. Mater. Interfaces* **4,** 4231–4236 (2012).
30. Li, X. B. *et al.* Controllable Low-Temperature Chemical Vapor Deposition Growth and Morphology Dependent Field Emission Property of $SnO_2$ Nanocone Arrays with Different Morphologies. *ACS Appl. Mater. Interfaces* **5,** 3033–3041 (2013).
31. Basu, S. *et al.* Fast Response Time Alcohol Gas Sensor Using Nanocrystalline F-Doped $SnO_2$ Films Derived via Sol-Gel Method. *Bull. Mater. Sci.* **36,** 521–533 (2013).
32. Moon, H. G. *et al.* Extremely Sensitive and Selective NO Probe Based on Villi-like $WO_3$ Nanostructures for Application to Exhaled Breath Analyzers. *ACS Appl. Mater. Interface* **5,** 10591–10596 (2013).
33. Wang, L. L. *et al.* Three-Dimensional Hierarchical Flowerlike $\alpha$-$Fe_2O_3$ Nanostructure: Synthesis and Ethanol-Sensing Properties. *ACS Appl. Mater. Interfaces* **3,** 4689–4694 (2011).
34. Lou, Z. *et al.* Branch-like Hierarchical Heterostructure ($\alpha$-$Fe_2O_3$/$TiO_2$): A Novel Sensing Material for Trimethylamine Gas Sensor. *ACS Appl. Mater. Interfaces* **5,** 12310–12316 (2013).
35. Zhang, F. H. *et al.* Controlled Synthesis and Gas-Sensing Properties of Hollow Sea Urchin-like $\alpha$-$Fe_2O_3$ nanostructures and$\alpha$-$Fe_2O_3$ nanocubes. *Sens. Actuators B: Chem.* **141,** 381–389 (2009).
36. Singh, N. *et al.* Gold-Nanoparticle-Functionalized $In_2O_3$ Nanowires as CO Gas Sensors with a Significant Enhancement in Response. *ACS Appl. Mater. Interfaces* **3,** 2246–2252 (2011).
37. Fu, J. C. *et al.* Enhance Gas Sensing Performance of Electrospun Pt-Functionalized NiO Nanotubes with Chemical and Electronic Sensitization. *ACS Appl. Mater. Interfaces* **5,** 7410–7416 (2013).
38. Zhu, G. X. *et al.* Platelet-like Nickle Hydroxide: Synthesis and the Transferring to Nickel Oxide as A Gas Sensor. *Sens. Actuators B: Chem.* **412,** 100–106 (2013).
39. Cho, N. G. *et al.* Gas Sensing Properties of *p*-type Hollow NiO Hemispheres Prepared by Polymeric Colloidal Templating Method. *Sens. Actuators B: Chem.* **155,** 366–371 (2011).
40. Zhu, G. X. *et al.* Facile Fabrication and Enhanced Sensing Properties of Hierarchically Porous CuO Architectures. *ACS Appl. Mater. Interfaces* **4,** 744–751 (2012).
41. Zhang, Y. M. *et al.* Improvement of Response to Formaldehyde st Ag-$LaFeO_3$ Based Gas Sensors Through Incorporation of SWCNTs. *Sens. Actuators B: Chem.* **195,** 509–514 (2014).
42. Lv, Y. Y. *et al.* MOF-Templated Synthesis of Porous $Co_3O_4$ Concave Nanocubes with High Specific Surface Area and Their Gas Sensing Properties. *ACS Appl. Mater. Interfaces* **6,** 4186–4195 (2014).
43. Yoon, J.–W. *et al.* Design of a Highly Sensitive and Selective $C_2H_5OH$ Sensor Using p-Type $Co_3O_4$ Nanofiber. *Sens. Actuators B: Chem.* **161,** 570–577 (2012).
44. Wen, Z. *et al.* Rhombus-Shaped $Co_3O_4$ Nanorod Arrays for High-Performance Gas Sensor. *Sens. Actuators B: Chem.* **186,** 172–179 (2013).
45. Choi, K. I. *et al.* $C_2H_5OH$ Sensing Characteristics of Various $Co_3O_4$ Nanostructures Prepared by Solvothermal. *Sens. Actuators B: Chem.* **146,** 183–189 (2010).
46. Kim, H. J. & Lee, J. H. Highly Sensitive and Selective Gas Sensors Using p-type Oxide Semiconductors: Overreview. *Sens. Actuators B: Chem.* **192,** 607–627 (2014).
47. Pirkanniemi, K. & Sillanpää, M. Heterogeneous water phase catalysis as an environmental application: a review. *Chemosphere*, **48,** 1047–1060 (2002).
48. Bettahar, M. M. *et al.* On the partial oxidation of propane and propylene on mixed metal oxide catalysts. *Appl.Catal. A: Gen.* **145,** 1–48 (1996).
49. Motooka, Y. & Ozaki, A. Regularities in catalytic properties of metal oxides in propylene oxidation. *J. Catal.* **5,** 116–124 (1966).
50. Kaye, S. S. & Long, J. R. Hydrogen storage in the dehydrated Prussian blue analogues M-3[Co(CN)(6)](2) (M = Mn, Fe, Co, Ni, Cu, Zn). *J. Am. Chem. Soc.* **127,** 6506–6507 (2005).
51. Bao, S. B. *et al.* Ultrafast Atomic Layer-by-Layer Oxygen Vacancy-Exchange Diffusion in Double-Perovskite $LnBaCo_2O_{5.5+\delta}$ Thin Films. *Sci. Rep.* **4,** 4726 (2014).
52. Wang, H. B. *et al.* Ultrafast Chemical Dynamic Behavior in Highly Epitaxial $LaBaCo_2O_{5+\delta}$ Thin Films. *J.Mater. Chem. C* **2,** 5660–5666 (2014).
53. Liu, M. *et al.* Effects of Annealing Ambient on Electrical Properties of $LaBaCo_2O_{5.5+\delta}$ Thin Films. *J. Nano Research* **27,** 25–30 (2014).

54. Hübner, M. & Simion, C. E. Influence of Humidity on CO Sensing with p-type CuO Thick Film Gas Sensors. *Sens. Actuators B: Chem*. **153,** 347–353 (2011).
55. Guo, Y. *et al.* Fabrication of (Calcein-ZnS)(n) Ordered Ultrathin Films on the Basis of Layered Double Hydroxide and Its Ethanol Sensing Behavior. *Ind. Eng. Chem. Res.* **51,** 8966–8973 (2012).

## Acknowledgements

This research was supported by the Natural Science Foundation of China (Nos. 51202185, 51390472, 51471169 and 11028409), the Fundamental Research Funds for the Central University, the National Science Foundation under NSF-NIRT-0709293, the U.S. Department of Energy under DE-FE0003780, and the State of Texas through the Texas Center for Superconductivity at the University of Houston. Moreover, M. Y. wants to acknowledge the Foundation of Shaanxi Educational Committee (14JK1331). The ethanol sensing properties of the LBCO thin films were measured using the GS-1TP intelligent gas sensing analysis system at Beijing Elite Tech. Co. Ltd., China, the authors also thank Ms. Dongmei Xu and Dr. Qi Qi for their help in gas-sensing property measurements.

## Author Contributions

M.L. and C.C. designed and setup the research, M.L. and S.R. prepared film samples, M.L., S.R. and R.Z. performed the structural characterization by HRXRD, C.M., Z.X., X.X., M.Y. and S.B. performed the electrical characterization. M.L., C.M. and C.C. analyzed the data and co-wrote the paper. All contributed discussion.

## Additional Information

**Competing financial interests:** The authors declare no competing financial interests.

**How to cite this article**: Liu, M. *et al.* Gas Sensing Properties of Epitaxial $LaBaCo_2O_{5.5+\delta}$ Thin Films. *Sci. Rep.* **5**, 10784; doi: 10.1038/srep10784 (2015).